Adjustable Discretized Population Balance for Growth and Aggregation

J. D. Litster, D. J. Smit, and M. J. Hounslow
Dept. of Chemical Engineering, University of Cambridge, Cambridge, CB2 3RA, UK

The discretized population balance (DPB) of Hounslow et al. (1988) is extended to allow the use of an adjustable discretization of the size domain of the form $v_{i+1}/v_i = 2^{1/q}$ (where $q \geq 1$ and is an integer). All the advantages of Hounslow et al.'s original work are retained: the zeroth and third moments of the particle-size distribution are correctly predicted, and the DPB is simple to solve with no integration within each size interval. The predicted and analytical particle size distributions are in excellent agreement for the cases of nucleation and growth and aggregation alone in batch and in continuous vessels. High-order moments and self-preserving particle-size distributions are accurately predicted when $q \geq 4$.

Introduction

The mathematical description of systems where nucleation, growth, and aggregation occur is referred to as the population balance (PB). The PB often takes the form of a nonlinear integro-partial-differential equation and is rarely analytically tractable.

A useful numerical technique for solving the PB is to discretize the particle-size domain into intervals and assume that the particle-size distribution (PSD) function is constant within each of these intervals. The resulting formulation is referred to as a discretized population balance (DPB) and is often simple to solve; integrals are just replaced with summations. DPBs have been developed by Gelbard and Seinfeld (1980), Batterham et al. (1981), Marchal et al. (1988), and Landgrebe and Pratsinis (1990). These DPBs vary in their choice of discretization (linear, geometric, arbitrary), their assumptions about the shape of the size distribution within each interval, and their choice of average values of properties for each interval. Hounslow (1990a) showed that some of the DPBs gave significant errors in their prediction of either total number or volume of particles. In general, the most accurate DPBs are also the most tedious to solve numerically, with many integrations within each size interval.

Hounslow et al. (1988) and Hounslow (1990b) also developed a DPB that has the advantage of being simple to solve as well as ensuring the correct prediction of total particle number and volume. A drawback of the DPB of Hounslow et al. is that it *fixes* the discretization of the size domain at $v_{i+1}/v_i = 2$. In practice, it is frequently desirable to use a much finer discretization. For example, devices that use electrical conductivity or light scattering to measure the PSD frequently obtain their measurements with a greater resolution than the discretization used by Hounslow et al. Additionally, as we shall show in this article, the DPB of Hounslow et al. results in considerable error in high-order moments of the PSD and subsequently, the prediction of the shape of the PSD is somewhat in error. The accurate prediction of the shape of the PSD is important, for example, when it is being used to deduce the aggregation mechanism (Ilievski et al., 1993).

In this article, we extended the approach of Hounslow et al. to an *adjustable* geometric size discretization of form $v_{i+1}/v_i = 2^{1/q}$, where q is an integer greater than or equal to one. We test the accuracy of the solutions at different values of q for four case studies: (I) aggregation only in a batch vessel; (II) aggregation only in a continuous well-mixed tank with representative overflow (CST); (III) nucleation and growth, and the growth of a charge in a batch vessel; (IV) nucleation and growth in a CST.

Theory

Population balance

The PB is a statement of continuity for particulate systems. It follows the change in the PSD as particles are born, die,

Present address of J. D. Litster: Department of Chemical Engineering, University of Queensland, Queensland, Australia.
Correspondence concerning this article should be addressed to M. J. Hounslow.

grow, or leave the control volume. The number of particles in the size range L to $L+dL$ is $n(L)dL$, where $n(L)$ is the population density function. Here L is some characteristic length of a particle. Later in this article we also use v, the volume of the particle as a measure of the particle size. In terms of $n(L)$, the unsteady state PB for a control volume is (Randolph and Larson, 1988)

$$\frac{\partial n}{\partial t}+\frac{\partial(Gn)}{\partial L}=B-D+\frac{1}{V}\left(\Sigma Q_{\text{in}}n_{\text{in}}-\Sigma Q_{\text{out}}n_{\text{out}}\right). \quad (1)$$

Equation 1 relates the accumulation of particles of a given size, $\partial n/\partial t$; the convective flux along the size axis, $\partial(Gn)/\partial L$; the birth and death rates, B and D; the bulk flow into and out of the control volume. G is the growth rate, dL/dt, and may be a function of size.

The birth and death terms cover discrete events such as nucleation, aggregation, and breakage. The birth and death terms for aggregation are, in terms of length, L

$$B(L)=\frac{L^2}{2}\int_0^L \frac{\beta((L^3-\lambda^3)^{1/3},\lambda)n((L^3-\lambda^3)^{1/3})n(\lambda)\,d\lambda}{(L^3-\lambda^3)^{2/3}} \quad (2)$$

$$D(L)=n(L)\int_0^\infty \beta(L,\lambda)n(\lambda)\,d\lambda. \quad (3)$$

Here $\beta(L,\lambda)$ is an aggregation rate constant called the kernel and may be a function of size. The following four case studies used in this paper result in particular forms of the PB.

Case Study I. Aggregation only in a batch vessel

$$\frac{dn(L)}{dt}=B(L)-D(L). \quad (4)$$

Case Study II. Aggregation only in an CST

$$\frac{n(L)-n_{\text{in}}(L)}{\tau}=B(L)-D(L). \quad (5)$$

Case Study III. Nucleation and size-independent growth in a batch vessel

$$\frac{dn(L)}{dt}+G\frac{d(n(L))}{dL}=B_0\delta(L). \quad (6)$$

Case Study IV. Nucleation and size-independent growth in an CST

$$\frac{n(L)-n_{\text{in}}(L)}{\tau}+G\frac{d(n(L))}{dL}=B_0\delta(L). \quad (7)$$

The moments of the PSD, at any time, are defined by

$$m_j=\int_0^\infty L^j n(L)\,dL. \quad (8)$$

Here m_0 is the total number of particles and m_3 is proportional to the total volume of particulate material. The sixth moment, m_6, is important in the prediction of mathematical gelation (Smit et al., 1994) and in the analysis of aerosol PSDs by light scattering techniques (Zachariah et al., 1989). While Eq. 1 can seldom be solved analytically, the moments of the PSD may occasionally be obtained. For example, for Case Study I, multiplying both sides of Eq. 4 by L^j and integrating with respect to L yields

$$\frac{dm_j}{dt}=\overline{B}_j-\overline{D}_j. \quad (9)$$

After application of Eq. 8 to Eqs. 2 and 3 and some simplification we get

$$\overline{B}_j-\overline{D}_j=\frac{1}{2}\int_0^\infty\int_0^\infty((L^3+\lambda^3)^{j/3}-L^j-\lambda^j)\beta(L,\lambda)n(L)n(\lambda)\,dL\,d\lambda. \quad (10)$$

For the size-independent kernel, $\beta(L,\lambda)=\beta_0$, and from Eqs. 9 and 10 we obtain that

$$\frac{dm_0}{dt}=-\frac{1}{2}\beta_0 m_0^2. \quad (11)$$

We also note from Eqs. 9 and 10 that Eq. 4 predicts the conservation of the total volume of particulate material for any kernel

$$\frac{dm_3}{dt}=0. \quad (12)$$

We use Eqs. 11 and 12 to test the predicted moments from the DPB.

Hounslow's original DPB

Hounslow et al. (1988) and Hounslow (1990b) produced a discretized form of the PB for both batch and CST vessels. In this approach the PSD is broken up into discrete size intervals using a geometric discretization of the form

$$\frac{v_{i+1}}{v_i}=2. \quad (13)$$

Here v_i is the lower bound of the ith interval in volume coordinates. The equivalent of Eq. 13 in terms of length is $L_{i+1}/L_i=2^{1/3}$.

We refer to aggregation events between particles in different intervals as interactions. By counting interactions that added to and removed particles from the ith interval, Hounslow et al. derived the following discretization for the birth and death terms due to aggregation

$$\left(\frac{dN_i}{dt}\right)_{\text{agg}}=\sum_{j=1}^{i-2}C\cdot 3\cdot 2^{j-i}\beta_{i-1,j}N_{i-1}N_j+\frac{1}{2}\beta_{i-1,i-1}N_{i-1}^2-N_i\sum_{j=1}^{i-1}C\cdot 3\cdot 2^{j-i-1}\beta_{i,j}N_j-N_i\sum_{j=i}^{\infty}\beta_{i,j}N_j. \quad (14)$$

Here N_i is the number of particles in the ith interval and C is a volume correction factor. The factor $C \cdot 3 \cdot 2^{j-1}$ in the first term in Eq. 14 indicates that a proportion of the interactions between particles in the $i-1$th and jth intervals produce particles in the ith interval. A similar factor applies to the third term, which accounts for the removal of particles from the ith interval by aggregation with particles in the jth interval ($j < i$). Equation 14 gives the correct rate of change of total number of particles for any value of C (Eq. 11). However, the third moment predicted by Eq. 14 is consistent with Eq. 12 only when $C = 2/3$. The final DPB birth and death terms were then given as

$$\left(\frac{dN_i}{dt}\right)_{\text{agg}} = \sum_{j=1}^{i-2} 2^{j-i}\beta_{i-1,j}N_{i-1}N_j + \frac{1}{2}\beta_{i-1,i-1}N_{i-1}^2 - N_i \sum_{j=1}^{i-1} 2^{j-i-1}\beta_{i,j}N_j - N_i \sum_{j=i}^{\infty} \beta_{i,j}N_j. \quad (15)$$

Hounslow et al. also proposed a discretization of the growth term. For nucleation and growth in a batch vessel the following two-term discretization is used

$$\left(\frac{dN_i}{dt}\right)_{\text{growth}} = \frac{2G}{(r-1)L_i}(rN_{i-1} - N_i) \quad (16a)$$

where $r = L_{i+1}/L_i$ and is the geometric discretization ratio. Equation 16a correctly predicts the zeroth moment, but none of the other moments of the PSD. In all other situations the following three-term discretization is used

$$\left(\frac{dN_i}{dt}\right)_{\text{growth}} = \frac{2G}{(r+1)L_i}\left(\frac{r}{r^2-1}N_{i-1} + N_i - \frac{r}{r^2-1}N_{i+1}\right). \quad (16b)$$

Here the zeroth, first, and second moments of the PSD are correctly predicted. This expression is general for any r, but matches the discretization for aggregation (Eq. 13) when $r = 2^{1/3}$. Hounslow et al. also showed that the jth moment may be obtained from

$$m_j = \sum_i \left(\frac{1+r}{2}L_i\right)^j N_i. \quad (17)$$

A DPB for a $2^{1/q}$ geometric discretization

Despite its usefulness, the main problem with Hounslow's DPB is that it is restricted to the discretization given in Eq. 13. We will now extend this to the more general case

$$\frac{v_{i+1}}{v_i} = 2^{1/q}. \quad (18)$$

Here q is any integer greater than or equal to one and yields the geometric discretization illustrated in Figure 1.

In Hounslow et al.'s original work ($q = 1$) only interactions involving particles in the $i-1$th interval can produce a particle in the ith interval. For finer discretizations (i.e., where $q \geq 2$) this is no longer the case. We first establish the types of interactions that affect the number of particles in the ith interval. There are five possible types of interaction that change the number of particles in the ith interval. The three that add particles to the ith interval are:

Type 1. Some of the interactions give particles in the ith interval and some give particles smaller than the ith interval.

Type 2. All interactions give particles in the ith interval.

Type 3. Some interactions give particles in the ith interval and some give particles larger than the ith interval.

The two that remove particles from the ith interval are:

Type 4. Some interactions remove particles from the ith interval.

Type 5. All interactions remove particles from the ith interval.

By looking at the interactions involving particles bounding each interval we can tell which of these interactions fall into each of the preceding categories. Table 1 shows all the interactions that change the number of particles in the ith interval for values of q from 1 to 4. By inspection, the general case for any value of q is derived. The total birth and death terms due to aggregation are

$$\left(\frac{dN_i}{dt}\right)_{\text{agg}} = \sum_{j=1}^{i-S(q)-1} K_1\beta_{i-1,j}N_{i-1}N_j + \sum_{k=2}^{q}\sum_{j=i-S(q-k+2)-k+1}^{i-S(q-k+1)-k} K_2\beta_{i-k,j}N_{i-k}N_j + \frac{1}{2}\beta_{i-q,i-q}N_{i-q}^2 + \sum_{k=2}^{q}\sum_{j=i-S(q-k+2)-k+2}^{i-S(q-k+1)-k+1} K_3\beta_{i-k+1,j}N_{i-k+1}N_j - \sum_{j=1}^{i-S(q)} K_4\beta_{i,j}N_iN_j - \sum_{j=i-S(q)+1}^{\infty}\beta_{i,j}N_iN_j. \quad (19)$$

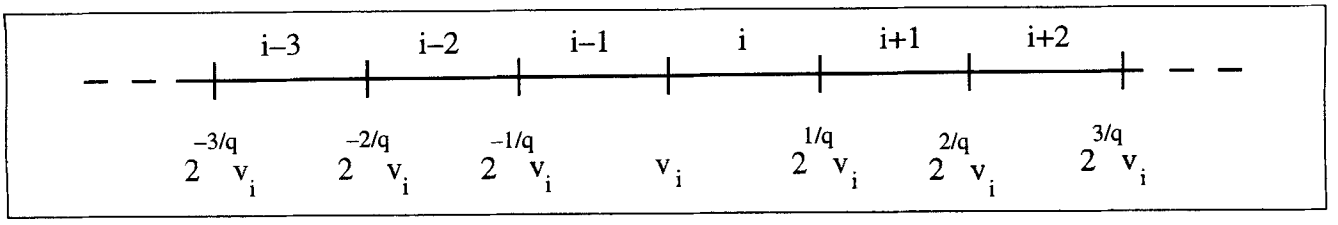

Figure 1. Discretization of the size domain.

Table 1. Interactions that Add to (Types 1, 2 and 3) and Remove from (Types 4 and 5) the Number of Particles in the ith Size Interval

		Size Interval 2				
q	Size Interval 1	Type 1 (Birth)	Type 2 (Birth)	Type 3 (Birth)	Type 4 (Death)	Type 5 (Death)
1	i	—	—	—	$1 \le j \le i-1$	$i \le j \le \infty$
	$i-1$	$1 \le j \le i-2$	$i-1$	—	—	—
2	i	—	—	—	$1 \le j \le i-3$	$i-2 \le j \le \infty$
	$i-1$	$1 \le j \le i-4$	—	$i-3 \le j \le i-2$	—	—
	$i-2$	$i-4 \le j \le i-3$	$i-2$	—	—	—
3	i	—	—	—	$1 \le j \le i-6$	$i-5 \le j \le \infty$
	$i-1$	$1 \le j \le i-7$	—	$i-6 \le j \le i-4$	—	—
	$i-2$	$i-7 \le j \le i-5$	—	$i-4 \le j \le i-3$	—	—
	$i-3$	$i-5 \le j \le i-4$	$i-3$	—	—	—
4	i	—	—	—	$1 \le j \le i-10$	$i-9 \le j \le \infty$
	$i-1$	$1 \le j \le i-11$	—	$i-10 \le j \le i-7$	—	—
	$i-2$	$i-11 \le j \le i-8$	—	$i-7 \le j \le i-5$	—	—
	$i-3$	$i-8 \le j \le i-6$	—	$i-5 \le j \le i-4$	—	—
	$i-4$	$i-6 \le j \le i-5$	$i-4$	—	—	—
q	i	—	—	—	$1 \le j \le i-S(q)$	$i-S(q)+1 \le j \le \infty$
	$i-1$	$1 \le j \le i-S(q)-1$	—	$i-S(q) \le j \le i-S(q-1)-1$	—	—
	$i-2$	$i-S(q)-1 \le j \le i-S(q-1)-2$	—	$i-S(q-1)-1 \le j \le i-S(q-2)-2$	—	—
	$i-3$	$i-S(q-1)-2 \le j \le i-S(q-2)-3$	—	$i-S(q-2)-2 \le j \le i-S(q-3)-3$	—	—
	⋮	⋮	⋮	⋮	⋮	⋮
	$i-q$	$i-S(2)-q+1 \le j \le i-S(1)-q$	$i-q$	—	—	—

Here we define $S(q) = \sum_{p=1}^{q} p$. For each term, $\beta_{i,j} N_i N_j$ is the total rate of interactions between the ith and jth intervals. Where not all the interactions add to or remove from the ith interval, the constants K_1, K_2, K_3, and K_4 are the fraction of events that do. The second part of the derivation of the DPB is to determine the value of these constants. To do this we will follow the procedure previously used by Hounslow et al. for $q = 1$ and use a similar nomenclature. We arbitrarily choose $v_1 = 2^{1/q}$. Then the ith interval is defined as $2^{i/q} < v < 2^{(i+1)/q}$.

Type 1 Interactions

Consider interactions between particles in the $i-p$th and jth intervals where some give particles in the ith interval and some particles are too small. A particle of size between a and $a+da$ in the jth interval must aggregate with a particle in the size range $2^{i/q} - a < v < 2^{(i-p+1)/q}$ from the $i-p$th interval to give a particle in the ith interval. The rate of formation of particles in the ith interval by such interactions is

$$dR^{[1]}_{i-p,j} = \beta_{i-p,j} \frac{2^{(i-p+1)/q} - 2^{i/q} + a}{2^{(i-p+1)/q} - 2^{(i-p)/q}} N_{i-p} \frac{da}{2^{(j+1)/q} - 2^{j/q}} N_j$$

$$= \beta_{i-p,j} N_{i-p} N_j \frac{2^{(i-p+1)/q}(1 - 2^{(p-1)/q}) + a}{2^{(i+j-p)/q}(2^{1/q} - 1)^2} da. \quad (20)$$

Integrating to get the total rate for successful interactions between the $i-p$th and jth intervals

$$R^{[1]}_{i-p,j} = \frac{\beta_{i-p,j} N_{i-p} N_j}{2^{(i+j-p)/q}(2^{1/q} - 1)^2} \int_{2^{i/q}}^{2^{(j+1)/q}} (2^{(i-p+1)/q}(1 - 2^{(p-1)/q}) + a)\, da$$

$$= \frac{\beta_{i-p,j} N_{i-p} N_j}{(2^{1/q} - 1)} \left(2^{1/q}(1 - 2^{(p-1)/q}) + \frac{2^{1/q} + 1}{2} 2^{(j-i+p)/q} \right). \quad (21)$$

Comparison of Eq. 21 and terms 1 and 2 of Eq. 19 yields

$$K_1 = \frac{2^{1/q} + 1}{2(2^{1/q} - 1)} 2^{(j-i+1)/q} \quad (22)$$

$$K_2 = \frac{2^{1/q} - 2^{k/q}}{2^{1/q} - 1} + \frac{2^{1/q} + 1}{2(2^{1/q} - 1)} 2^{(j-i+k)/q}. \quad (23)$$

Type 2 Interactions

From Table 1, the only combination for which all interactions give particles in the ith interval is when both particles are from the $i-q$th interval. It then follows that

$$R^{[2]}_{i-q,i-q} = \frac{1}{2} \beta_{i-q,i-q} N^2_{i-q}. \quad (24)$$

The factor 1/2 ensures that each interaction is not counted twice.

Type 3 Interactions

Consider interactions between particles in the $i-p$th and jth intervals where some of the resulting particles fall into

the ith interval and some are too large. A particle of size between a and $a+da$ in the jth interval must aggregate with a particle in the size range $2^{(i-p)/q} < v < 2^{(i+1)/q} - a$ from the $i-p$th interval to give a particle in the ith interval. The rate of formation of particles in the ith interval by such collisions is

$$dR^{[3]}_{i-p,j} = \beta_{i-p,j} N_{i-p} N_j \frac{2^{(i+1)/q} - 2^{(i-p)/q} - a}{2^{(i+j-p)/q}(2^{1/q}-1)^2} da. \quad (25)$$

Integrating to get the total rate of successful interactions between the $i-p$th and jth intervals

$$R^{[3]}_{i-p,j} = \frac{\beta_{i-p,j} N_{i-p} N_j}{2^{1/q}-1}\left((2^{(p+1)/q}-1) - \frac{2^{1/q}+1}{2} 2^{(j-i+p)/q}\right). \quad (26)$$

Comparison of Eq. 26 with term 4 of Eq. 19 yields

$$K_3 = \frac{2^{k/q}-1}{2^{1/q}-1} - \frac{(2^{1/q}+1)}{2(2^{1/q}-1)} 2^{(j-i+k-1)/q}. \quad (27)$$

Type 4 Interactions

Consider interactions between particles in the ith and jth intervals where some remove particles from the ith interval. A particle of size between a and $a+da$ in the jth interval must interact with a particle in the size range $2^{(i+1)/q} - a < v < 2^{(i+1)/q}$ to remove this particle from the ith interval. The rate of removal of particles in the ith interval by such collisions is

$$dR^{[4]}_{i,j} = \frac{\beta_{i,j} N_i N_j a da}{2^{(i+j)/q}(2^{1/q}-1)^2}. \quad (28)$$

Integrating over all the jth interval yields

$$R^{[4]}_{i,j} = \beta_{i,j} N_i N_j \frac{2^{1/q}+1}{2(2^{1/q}-1)} 2^{(j-i)/q}. \quad (29)$$

Comparing Eq. 29 with term 5 of Eq. 19 yields

$$K_4 = \frac{(2^{1/q}+1)}{2(2^{1/q}-1)} 2^{(j-i)/q}. \quad (30)$$

Type 5 Interactions

All combinations are successful in removing particles from the ith interval, and consequently,

$$R^{[5]}_{i,j} = \beta_{i,j} N_i N_j. \quad (31)$$

Substituting Eqs. 22, 23, 27, and 30 into Eq. 19 yields the following DPB

$$\left(\frac{dN_i}{dt}\right)_{\text{agg}} = \sum_{j=1}^{i-S(q)-1} \beta_{i-1,j} N_{i-1} N_j \left(\frac{2^{1/q}+1}{2(2^{1/q}-1)} 2^{(j-i+1)/q} + C_1\right) + \sum_{k=2}^{q} \sum_{j=i-S(q-k+1)-k}^{i-S(q-k+2)-k+1} \beta_{i-k,j} N_{i-k} N_j \left(\frac{2^{1/q}-2^{k/q}}{2^{1/q}-1} + \frac{2^{1/q}+1}{2(2^{1/q}-1)} 2^{(j-i+k)/q} + C_2\right) + \frac{1}{2}\beta_{i-q,i-q} N^2_{i-q} + \sum_{k=2}^{q} \sum_{j=i-S(q-k+1)-k+1}^{i-S(q-k+2)-k+2} \beta_{i-k+1,j} N_{i-k+1} N_j \left(\frac{2^{k/q}-1}{2^{1/q}-1} - \frac{(2^{1/q}+1)}{2(2^{1/q}-1)} 2^{(j-i+k-1)/q} - C_2\right) - \sum_{j=1}^{i-S(q)} \beta_{i,j} N_i N_j \left(\frac{(2^{1/q}+1)}{2(2^{1/q}-1)} 2^{(j-i)/q} + C_1\right) - \sum_{j=i-S(q)+1}^{\infty} \beta_{i,j} N_i N_j. \quad (32)$$

Here C_1 and C_2 are volume correction factors. As was the case in the development of Hounslow's original DPB, Eq. 32 correctly predicts the rate of change of the zeroth moment given by Eq. 11 for all values of C_1 and C_2. This is not the case for the third moment. That the third moment is not correctly predicted is a direct result of the problems of discretization. For example, consider a particle in the jth interval that interacts with a particle in the ith interval to produce a particle that is still in the ith interval. This interaction has not changed the number of particles in the ith interval and is not counted in Eq. 32. However, it has changed the volume of particulate material in the ith interval. In other words, we require the volume correction factors, C_1 and C_2, to account for those interactions that do not affect the zeroth moment of the ith interval, but do affect all the other moments in the ith interval. We show in the Appendices that when

$$C_1 = -\frac{2^{(j-i+1)/q}}{2} \quad (33)$$

and

$$C_2 = \frac{-2^{(j-i+1)/q}}{2^{1/q}-1}\left(\frac{2^{1/q}+1}{2} 2^{(k-1)/q} - 1\right) + \frac{2^{-(k-1)/q} + 2^{k/q} - 2^{1/q} - 1}{2^{1/q}-1}, \quad (34)$$

then Eq. 32 predicts the correct rate of change of both the zeroth and the third moments. Substituting Eqs. 33 and 34 into Eq. 32 gives the final modified DPB for aggregation

$$\left(\frac{dN_i}{dt}\right)_{agg} = \sum_{j=1}^{i-S(q)-1} \beta_{i-1,j} N_{i-1} N_j \frac{2^{(j-i+1)/q}}{2^{1/q}-1}$$

$$+ \sum_{k=2}^{q} \sum_{j=i-S(q-k+2)-k+1}^{i-S(q-k+1)-k} \beta_{i-k,j} N_{i-k} N_j \frac{2^{(j-i+1)/q} - 1 + 2^{-(k-1)/q}}{2^{1/q}-1}$$

$$+ \frac{1}{2}\beta_{i-q,i-q} N_{i-q}^2$$

$$+ \sum_{k=2}^{q} \sum_{j=i-S(q-k+2)-k+2}^{i-S(q-k+1)-k+1} \beta_{i-k+1,j} N_{i-k+1} N_j \frac{-2^{(j-i)/q} + 2^{1/q} - 2^{-(k-1)/q}}{2^{1/q}-1}$$

$$- \sum_{j=1}^{i-S(q)} \beta_{i,j} N_i N_j \frac{2^{(j-i)/q}}{2^{1/q}-1}$$

$$- \sum_{j=i-S(q)+1}^{\infty} \beta_{i,j} N_i N_j. \qquad (35)$$

Equation 35 reduces to Hounslow et al.'s (1988) original DPB when $q = 1$. Note that for $q \geq 2$, two extra summation terms are the only changes necessary in the DPB. Unlike the DPB of Gelbard and Seinfeld (1980) and Landgrebe and Pratsinis (1990), no integration within each interval is required. We now proceed to test the discretization for growth and aggregation in both batch and CST vessels.

Case Study I: Aggregation Only in a Batch Vessel

In all case studies, the DPB is tested by comparing the numerical results with known analytical solutions of the PB. Hounslow et al. (1988) and Hounslow (1990b) have demonstrated examples where the DPB with $q = 1$ gives good agreement with analytical solutions. In this paper, we make more demanding tests of the DPB to highlight conditions where a finer discretization is necessary to reduce the errors in the predicted size distributions. Large relative errors are most likely in the tail of the PSD and at high extents of aggregation. For this reason, particle-size distributions are presented as cumulative oversize distributions on a logarithmic scale. Results are presented at high extents of aggregation, typically $I_{agg} \geq 0.95$, where I_{agg} is defined as

$$I_{agg} = 1 - \frac{m_0}{m_0^{\phi}}.$$

Here m_0^{ϕ} is the zeroth moment of the charge in the batch vessel. The zeroth to sixth moments of the predicted PSDs are also compared to analytical solutions at high values of I_{agg}. This range covers all moments of practical importance.

In testing the model at different values of q, values of the total number of equations, n_{eq}, were chosen such that the range of the finite domain remained constant, that is, such that n_{eq}/q remained constant. For batch vessels, the discretization of aggregation, Eq. 35, results in a set of ordinary differential equations made up of simple summation terms. These ODEs were solved using the NAG library routine D02NBF.

Size-independent aggregation

For the case where $\beta(L, \lambda) = \beta_0$ and where the PSD of the charge in the batch vessel is given by

$$n(x) = \frac{N_0}{v_0} \exp(-x), \qquad (36)$$

Gelbard and Seinfeld (1978) provide the following analytical solution

$$n(x) = \frac{4N_0}{v_0(Y+2)^2} \exp\left(-\frac{2x}{(Y+2)}\right). \qquad (37)$$

Here $Y = N_0 \beta_0 t$ and $x = v/v_0$. The cumulative oversize number and volume fractions may be simply obtained from Eq. 37. They are

$$\text{COS } N(x) = \exp\left(-\frac{2x}{Y+2}\right) \qquad (38)$$

$$\text{COS } V(x) = \exp\left(-\frac{2x}{Y+2}\right)\left(1+\frac{2}{Y+2}\right). \qquad (39)$$

It follows from Eq. 37 that the dimensionless moments of the PSD are

$$\tilde{m}_j = \frac{m_j}{m_j|_{t=0}} = \left(\frac{2}{Y+2}\right)^{1-j/3} \qquad (40)$$

The numerical solution obtained from Eq. 35 is compared with Eqs. 38 and 39 in Figure 2 for $I_{agg} = 0.98$. In both these cases, solutions using the original Hounslow DPB ($q = 1$) differ considerably from the analytical solutions, with the numerically predicted cumulative volume distribution more in error than the cumulative number distribution. This is because the DPB is most in error at large particle sizes, where a small error in particle numbers has a large effect on particle volume. However, by $q = 3$, the DPB solution is in good agreement with the analytical solutions, Eqs. 38 and 39.

In Figure 3, the relative error in the second and sixth moments obtained from Eqs. 35 and 40 are plotted against I_{agg}. Note that the error in these moments decreases as q is increased and that the relative error increases as I_{agg} is increased. In Figure 4, the relative error in all the moments is given at different values of q for $I_{agg} = 0.98$. The zeroth and third moments are always correctly predicted and errors in the first and second moments are small, even for $q = 1$. For any given value of q, the sixth moment has the largest error. This is expected because the sixth moment weights the larger particles sizes where the DPB is most in error. By $q = 5$ all predicted moments (up to the sixth moment) have less than 1 percent error.

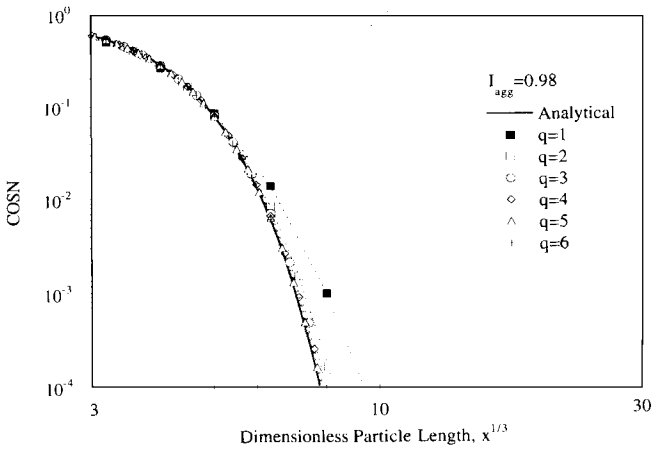

(a)

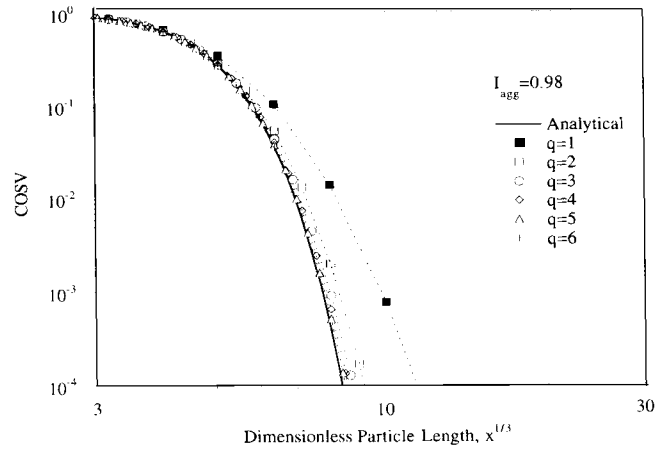

(b)

Figure 2. Size-independent aggregation of an exponential charge in a batch vessel.

Comparison of Eq. 35 with (a) Eq. 38 and (b) Eq. 39.

Another test of this DPB is its ability to predict the self-preserving PSD associated with the size-independent kernel. Friedlander (1977) has shown that for some kernels the PSD approaches a form at long times that is independent of the initial PSD. This self-preserving form is obtained by scaling the density function as follows

$$\psi(\eta) = n(v)\bar{v}/m_0. \tag{41}$$

Here $\eta = v/\bar{v}$ and $\bar{v} = m_3/m_0$. It is a simple matter to show from Eqs. 37 and 41 that for the size-independent kernel

$$\psi(\eta) = \exp(-\eta). \tag{42}$$

In Figure 5, we compare the results obtained from Eq. 35 with Eq. 42. For $q = 6$ the DPB prediction is indistinguishable from the analytical self-preserving PSD.

Size-dependent aggregation

We now consider the aggregation of the charge given by Eq. 36 for the kernel, $\beta(L, \lambda) = \beta_0(L^3 + \lambda^3)$. For this case, Gelbard and Seinfeld give the following analytical solution for the population density function

$$n(x) = \frac{N_0(1-T)}{v_0 x\sqrt{T}} \exp(-(1+T)x) I_1(2x\sqrt{T}). \tag{43}$$

Here $T = 1 - \exp(-Y)$ and I_1 is the modified Bessel function of the first kind of order one. In Figure 6, we compare cumulative number and volume distributions obtained from Eq. 43 with those obtained from Eq. 35 for $I_{agg} = 0.95$. The cumulative number distribution is well predicted by Eq. 35 for $q = 3$. However, there is still significant error in the predicted cumulative volume distribution for $q = 3$. The predicted cumulative volume distribution approaches the analytical solution only when $q = 6$.

In Figure 7, values of the moments of the PSD obtained from Eq. 43 are compared with those obtained from Eq. 35. As for the case of size-independent aggregation, the relative error is greatest for the sixth moment and decreases as q is increased. Figure 7 differs from Figure 4 in that the relative

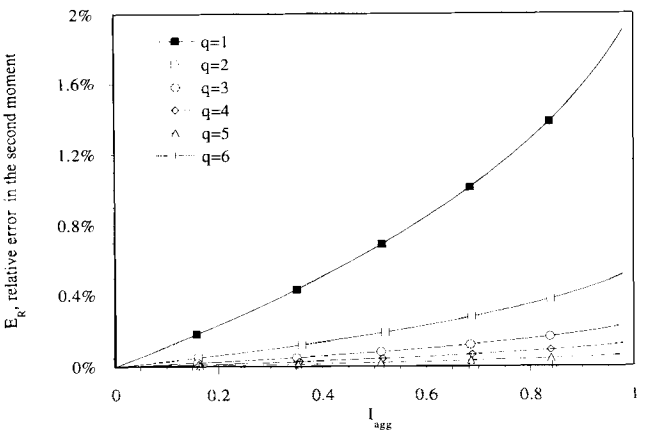

(a)

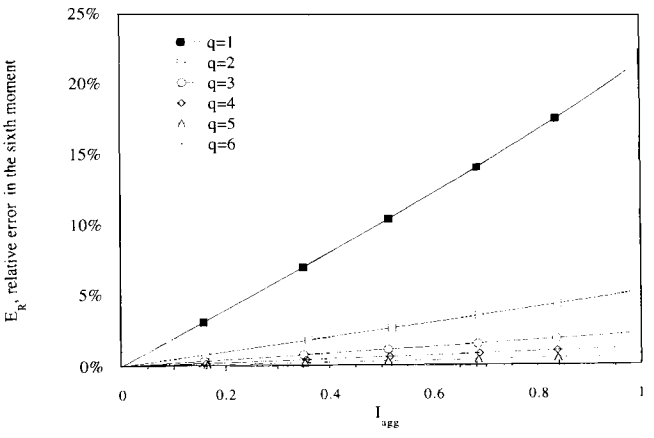

(b)

Figure 3. Size-independent aggregation of an exponential charge in a batch vessel.

Relative error in the DPB predicted (a) second and (b) sixth moments.

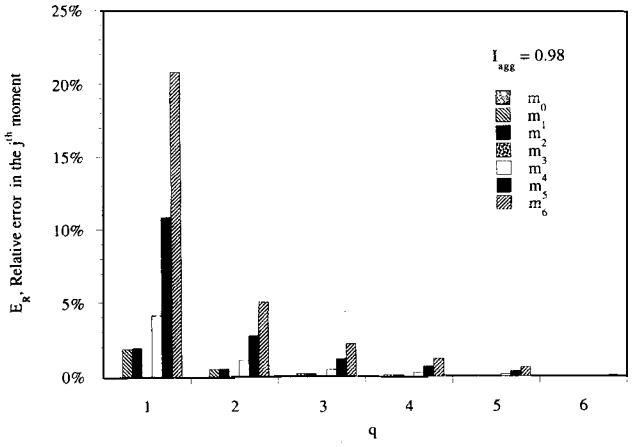

Figure 4. Relative error in the moments for the size-independent aggregation of an exponential charge in a batch vessel.

error in all the moments is much larger than for the size-independent aggregation. For example, for $q = 6$ the sixth moment has a relative error of approximately 7% (cf. 1 percent for size-independent aggregation).

Friedlander (1977) gives a numerical solution of the self-preserving PSD for the kernel, $\beta(L, \lambda) = (L + \lambda)(L^{-1} + \lambda^{-1})$. In Figure 8 we compare this solution to results obtained from Eq. 35 and note that, for $q = 9$, the DPB prediction is in excellent agreement with the self-preserving PSD given by Friedlander.

Landgrebe and Pratsinis (1990, Fig. 3b) have also tested their DPB for its ability to predict this self-preserving PSD. Those authors use the equivalent of values of q that range from $q \equiv 1$ to $q = 9$. At $q = 9$, Eq. 35 shows a comparable performance to their DPB but, unlike their DPB, does not require any integration within the intervals. Clearly, the success of Landgrebe and Pratsinis's DPB is due to the fine discretization, rather than the integration within each size interval at each time step.

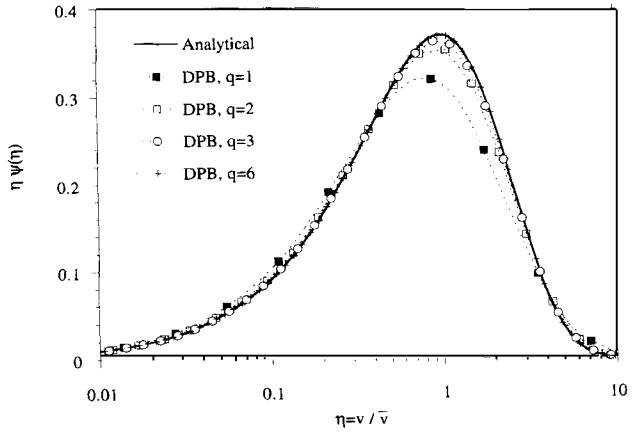

Figure 5. Self-preserving PSD for size-independent aggregation in a batch vessel.

Comparison of DPB, Eq. 35, and analytical, Eq. 42, solutions.

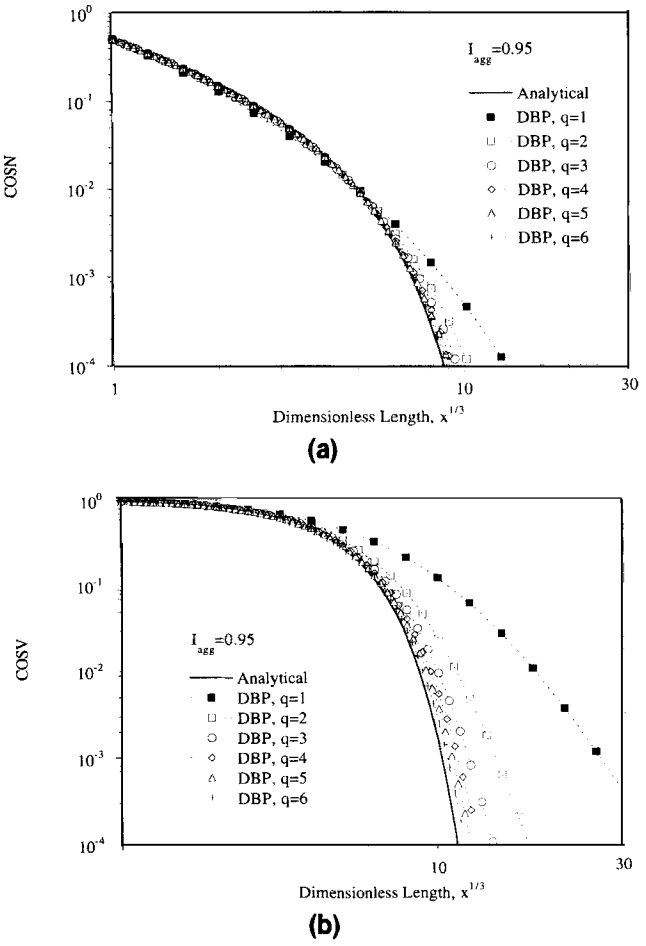

Figure 6. Size-dependent aggregation of an exponential charge in a batch vessel.

Comparison of the analytical (a) COSN and (b) COSV distributions, obtained from Eq. 43, with solutions obtained from the DPB, Eq. 35.

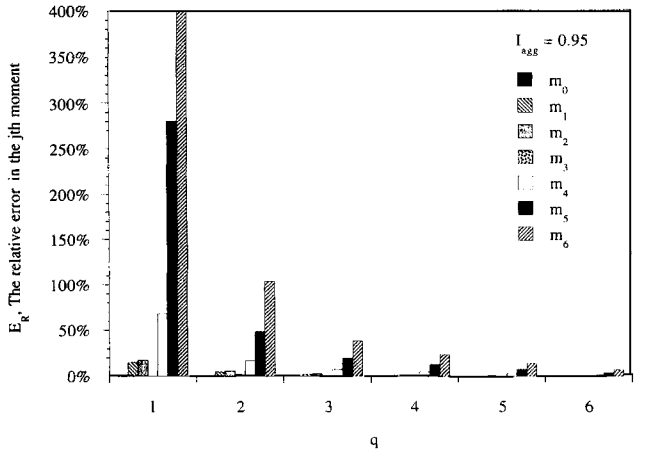

Figure 7. Relative errors in the moments for the size-dependent aggregation of an exponential charge in a batch vessel.

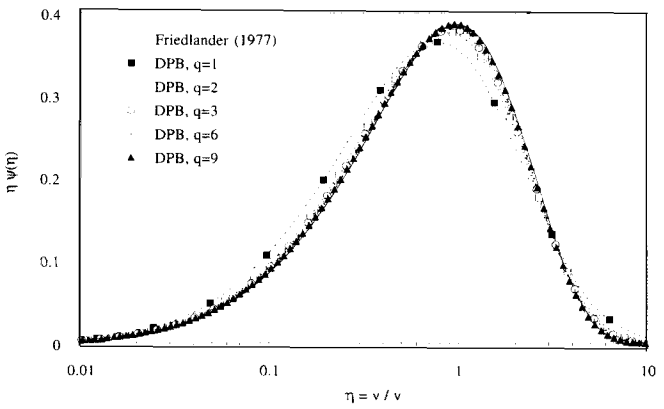

Figure 8. Self-preserving PSD for the kernel, $\beta(L, \lambda) = \beta_0(L+\lambda)(L^{-1}+\lambda^{-1})$ in a batch vessel.

On comparing Figure 2 with Figure 6, Figure 4 with Figure 7, and Figure 5 with Figure 8, it is clear that a greater value q is required for a size-dependent kernel than for the size-independent kernel before the numerical and analytical solutions are in good agreement. This is perhaps because the sum kernel, which is first order with respect to particle volume, weights large particle sizes where the geometric size distribution has the least number of data points. Note from Figures 5 and 8 that the size-independent and Brownian kernels, which are both zero-order kernels, have similar errors to one another at a given value of q. We propose that at a given value of q, the higher the order of the kernel, the greater the error in the DPB solution will be.

Case Study II: Aggregation only in a CST Vessel

Having considered size-independent and size-dependent aggregation for batch vessels, we now consider only size-independent aggregation in CST vessels. Hounslow (1990b) applies the discretization of aggregation for batch vessels to CST vessels as follows:

$$\frac{N_i - N_{i,\text{in}}}{\tau} = \left(\frac{dN_i}{dt}\right)_{\text{agg}} \tag{44}$$

Here the right of Eq. 44 is the result for batch aggregation, and is now obtained from Eq. 35. The PB for this case, Eq. 5, is now transformed into a set of nonlinear simultaneous equations that were solved using the NAG library routine C02PDF. For a feed to a CST given by Eq. 37 and where $\beta(L, \lambda) = \beta_0$, Hounslow (1990b) gives the following analytical solution

$$n(x) = \frac{N_0}{v_0} \frac{I_0((-Yx)/(1+2Y)) + I_1((-Yx)/(1+2Y))}{\exp(((1+Y)x)/(1+2Y))\sqrt{1+2Y}} \tag{45}$$

In Figure 9, the cumulative number and volume size distributions obtained by numerically integrating Eq. 45 are compared with solutions obtained from the CST form of the DPB, Eq. 44 for $I_{\text{agg}} = 0.994$. The cumulative number distribution is well predicted even for $q = 1$. However, a value of $q = 3$ is required before error in the predicted cumulative volume distribution is small.

In Figure 10, we consider the relative errors in the moments of the PSD obtained from Eqs. 44 and 45. The same trend as that for a batch vessel (Figure 4) is seen here. For $q = 6$, the relative error in the sixth moment is approximately 2 percent. The errors in the PSD for the batch and continuous cases are of the same order, provided they are compared at similar extents of aggregation.

Case Study III: Size-Independent Growth in a Batch Vessel

The original Hounslow discretization of growth was derived for an arbitrary geometric discretization, see Eq. 16. We now test this discretization at various values of q. For simultaneous growth and nucleation in a batch vessel the population balance is given by Eq. 6. The analytical solution for the PB is

$$n(L, t) = \frac{B_0}{G} u\left(t - \frac{L}{G}\right) \tag{46}$$

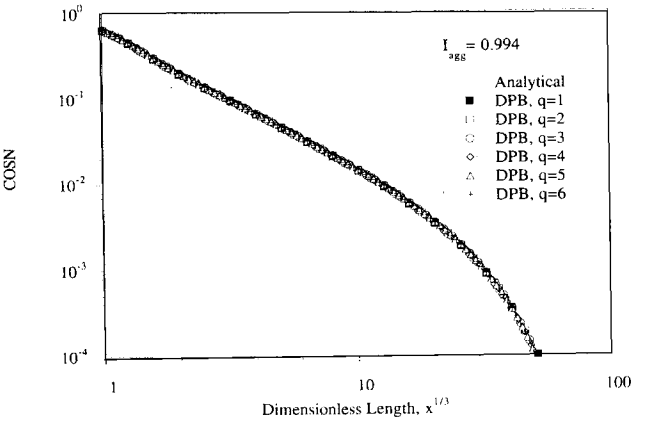

(a)

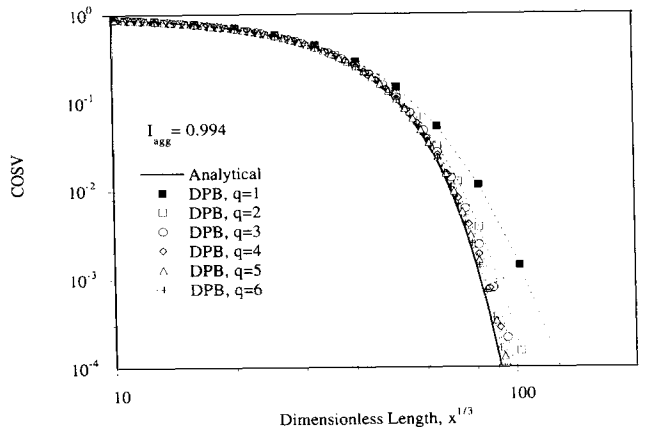

(b)

Figure 9. Size-independent aggregation of an exponential feed in a CST.

Comparison of the (a) cos N and (b) cos V PSDs obtained from Eq. 44 and Eq. 45.

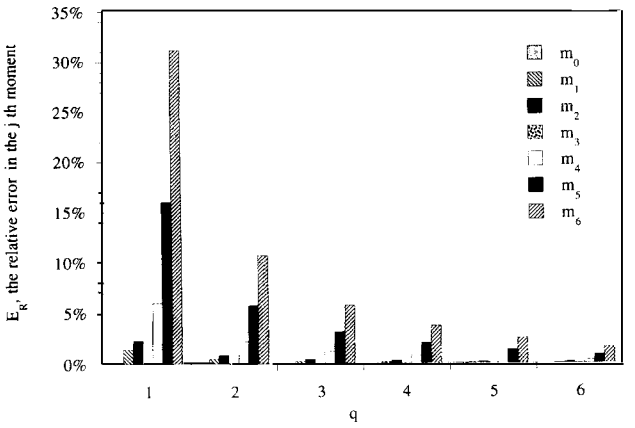

Figure 10. Size-independent aggregation of an exponential feed in a CST—Relative errors in the moments.

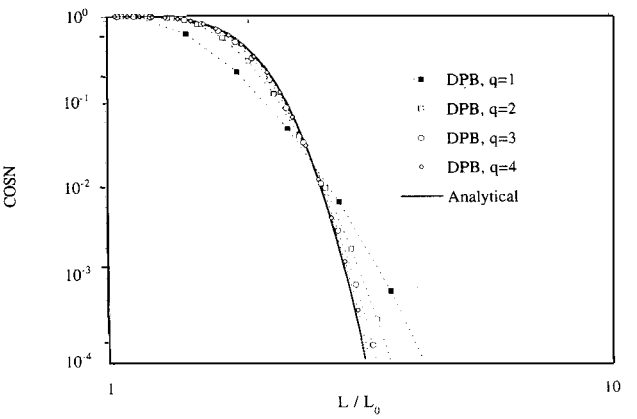

Figure 12. Size-independent growth of an exponential charge in a batch vessel.
Comparison of Eq. 16b and Eq. 47.

where u is the unit step function. In Figure 11, solutions obtained from Eq. 16a are compared with Eq. 46. The DPB was solved for the case of a constant growth rate ($G = 1$ length unit per unit time) and constant nucleation rate ($B_0 = 1$ per unit volume per unit time) after 10 units of time. The numerical solution is in good agreement with the exact solution despite the difficulty of predicting a (moving) discontinuity with discretized equations. As expected, the accuracy of the numerical solution improves as q is increased.

For the size-independent growth of a charge described by Eq. 36 the analytical solution is

$$\bar{n}(L,,t)\begin{cases} = 0, & L \le Gt \\ = \exp\left[-\left(\dfrac{L-Gt}{L_0}\right)^3\right], & L > Gt \end{cases} \quad (47)$$

Here L_0 corresponds to v_0 and $\bar{n}(L, t) = n(L, t)L_0/N_0$. Figure 12 shows a comparison of Eq. 47 with results from Eq. 16b when $Gt = L_0 = 1$. Clearly, while solutions for $q = 1$ are somewhat in error, these errors decrease as q is increased.

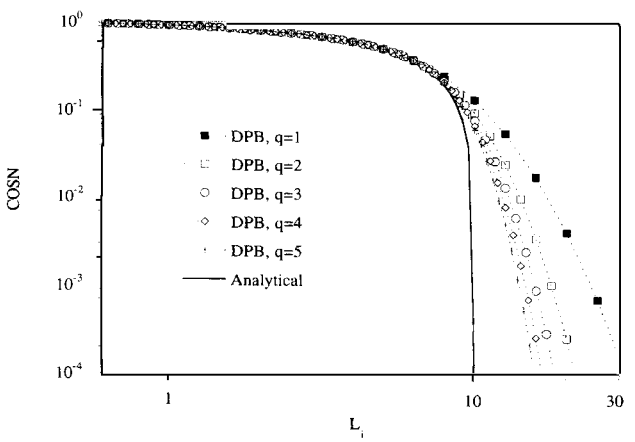

Figure 11. Nucleation and size-independent growth in a batch vessel.
Comparison of Eq. 16a and Eq. 46.

Case Study IV: Nucleation and Size-Independent Growth in a CST Vessel

For our final case study the solution to the PB, Eq. 7, is well known. Randolph and Larson (1988) give the following solution

$$\text{COS } V(z) = 1 - \exp(-z)\left(1 + z + \frac{z^2}{2} + \frac{z^3}{6}\right) \quad (48)$$

where $z = L/G\tau$. The discretization of growth and nucleation in a CST now becomes

$$\frac{N_i - N_{i,\text{in}}}{\tau} = \left(\frac{dN_i}{dt}\right)_{\text{growth}} + \left(\frac{dN_i}{dt}\right)_{\text{nucleation}} \quad (49)$$

Here the right of Eq. 49 is obtained from Eqs. 16b and

$$\left(\frac{dN_i}{dt}\right)_{\text{nucleation}} = \begin{cases} B_0, & i = 1 \\ 0, & i \ne 1 \end{cases}.$$

In Figure 13 a comparison is given between Eq. 48 and the cumulative volume distribution obtained from Eq. 49. The fit between the analytical and numerical solutions is good for $q \ge 4$.

For $q = 1$, Hounslow (1990b) gives values of the lower bound of the size domain that minimize the finite domain error. For arbitrary q this now becomes

$$z_1^{\text{opt}} = \frac{\dfrac{n_{\text{eq}}}{3q}\ln(2)}{2^{n_{\text{eq}}/3q} - 1}. \quad (50)$$

As is the case for $q = 1$, using these or larger values of z_1 avoids the oscillations in the numerical values of N_i (for $i \le 5$). This numerical artifact is fully discussed by Hounslow (1990b).

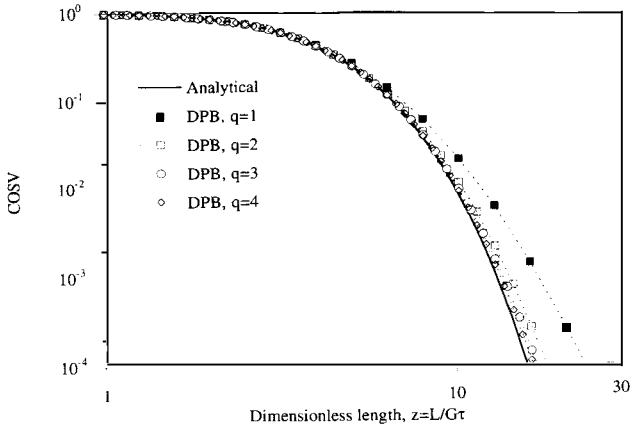

Figure 13. Nucleation and size-independent growth in a CST.

Comparison of Eq. 48 and Eq. 49.

For $q = 1$, Hounslow et al. note that the error in the predicted third moment is 1.8%. The relative error in the predicted third moment in terms of arbitrary q is given by

$$E_R = \frac{(2^{1/3q} - 1)^2}{3 \cdot 2^{1/3q}}. \tag{51}$$

From Eq. 51, it follows that the relative error in the third moment is always less than 0.45% for $q \geq 2$.

CPU Time

For some purposes, solving the DPB with a value of $q = 1$ gives numerical solutions that are sufficiently accurate; for example, when errors in the measured data are far larger than those in the numerical solution. However, for those cases where more accurate numerical solutions of the PB are required, a finer discretization (i.e., a larger value of q) should be used. The value of q used depends on the requirements of the users. If, for example, it is required that the sixth moment is predicted with less than one percent error, then a value of $q = 6$ is needed (see Figure 4).

A finer discretization, however, requires a larger number of intervals to cover the same finite domain. Thus increasing q implies an increase in both the value of n_{eq} and in the CPU time required to solve the DPB. In Table 2 we consider the increase in the CPU time required as q is increased for size-independent aggregation in a batch vessel when $n_{eq}/q =$ 20, 30, and 40 and $I_{agg} = 0.98$. Simulations were performed on a SUN SLC workstation.

Table 2. Relative CPU Times on a SUN SLC Workstation

	CPU time		
q	$(n_{eq}/q = 20)$	$(n_{eq}/q = 30)$	$(n_{eq}/q = 40)$
1	1	2.7	5.8
2	8	23.4	52.2
3	21	63.3	**140.6**
4	49.5	**148.1**	334.7
5	95.4	289.4	650
6	**167.7**	511	1077

Note: Data obtained for the case of size-independent aggregation in a batch vessel when $I_{agg} = 0.98$.

Note from Table 2 that the CPU time taken depends mainly on the number of intervals needed to cover the finite domain, that is, on n_{eq}. For all three cases of constant n_{eq}/q, computational requirements increase approximately with q^3. The error in the moments of the PSD, however, decreases at a slower rate, typically with $q^{-1.75}$. Consequently, a good trade-off between accuracy requirements and computational time is obtained when $q = 3$ or 4.

Consider the CPU times in Table 2 that are given in bold lettering. These are all for a value of $n_{eq} = 120$ but at different values of q. We note that, of itself, increasing the value of q has a little effect on the CPU time.

Conclusions

In this article we extend the DPB of Hounslow et al. (1988), allowing the use of an adjustable geometric discretization of the size domain such that $v_{i+1}/v_i = 2^{1/q}$. Here q is an integer greater than or equal to one. This DPB retains all the advantages of the original DPB in that it is simple to solve (e.g., requiring no integration within each interval) and correctly predicts the zeroth and third moments of the PSD.

Furthermore, it was found that at a sufficiently large value of q, the new DPB was able to predict correctly (1) cumulative number and volume distributions; (2) self-preserving PSDs; and (3) high-order moments of the PSD. The mechanisms of nucleation, (size-independent) growth, and (size-independent and size-dependent) aggregation were considered in both batch and continuous vessels at steady state.

It is suggested that a reasonable trade-off between accuracy and the increased computational time required to solve the DPB at increasing values of q may be obtained for a value of $q = 3$ or 4.

Acknowledgments

This work was supported by the Science and Engineering Research Council of Great Britain under its Specially Promoted Programme in Particle Technology (Grant Number GR/H28684). Dr. Litster thanks Prof. S. E. Pratsinis from the University of Cincinnati for many useful discussions on solutions to the PB and particularly for pointing out errors in the predicted self-preserving size distributions using Hounslow's DPB.

Notation

B_0 = nucleation rate
$\overline{B}, \overline{D}$ = moment form of the birth and death terms
B, D = birth and death terms
$C_{1,2}$ = volume correction factors
E_R = relative error
G = growth rate, dL/dt
K_{1-4} = fractions of interactions that add to or remove particles from the ith interval
L = length of a particle
m = moment of the PSD
N = number of particles per unit volume
n = population or number density function
n_{eq} = number of intervals used in the DPB

Q = flow rate
q = adjustable parameter determining value of r
r = geometric discretization factor, $L_{i+1}/L_i = 2^{1/3q}$
S = summation function, $S(q) = \sum_{p=1}^{q} p$
t = time
T = dimensionless variable
u = unit step function
v = volume of a particle
$\bar{v}$ = mean particle size, m_3/m_0
x = dimensionless particle volume, v/v_0
Y = dimensionless time, $N_0 \beta_0 t$
z = dimensionless length, L/Gt

Greek letters

$\beta(L, \lambda)$ = aggregation kernel
β_0 = size-independent part of the aggregation kernel
λ = particle length
η = dimensionless particle volume, $v/\bar{v}$
ψ = self-preserving PSD
τ = mean residence time

Superscripts and subscripts

$\sim$ = dimensionless moment
in = in the feed to a CST
j = jth moment
i = in the ith interval
ϕ = relating to the charge in a batch vessel

Literature Cited

Batterham, R. J., J. S. Hall, and G. Barton, "Pelletizing Kinetics and Simulation for Full-Scale Balling Circuits," *Proc. Int. Symp. on Agglomeration*, A136 (1981).

Friedlander, S. K., *Smoke, Dust and Haze*, Wiley, New York (1977).

Gelbard, F., and J. H. Seinfeld, "Numerical Solutions of the Dynamic Equation for Particulate Systems," *J. Comp. Phys.*, **28**, 357 (1978).

Gelbard, F., and J. H. Seinfeld, "Simulation of Multicomponent Aerosol Dynamics," *J. Colloid Interface Sci.*, **78**(2), 485 (1980).

Hounslow, M. J., R. L. Ryall, and V. R. Marshall, "A Discretized Population Balance for Nucleation, Growth, and Aggregation," *AIChE J.*, **34**(11), 1821 (1988).

Hounslow, M. J., "A Discretised Population Balance for Simultaneous Nucleation, Growth and Aggregation," PhD Thesis, Univ. of Adelaide, Adelaide, Australia (1990a).

Hounslow, M. J., "A Discretized Population Balance for Continuous Systems at Steady State," *AIChE J.*, **36**(1), 106 (1990b).

Ilievski, D., E. T. White, and M. J. Hounslow, "Agglomeration Mechanism Identification Case Study: $Al(OH)_3$ Agglomeration During Precipitation from Seeded Supersaturated Caustic Aluminate Solutions," Int. Symp. on Agglomeration, Nagoya, Japan (1993).

Landgrebe, J. D., and S. E. Pratsinis, "A Discrete-Sectional Model for Powder Production by Gas-Phase Chemical Reaction and Aerosol Coagulation in the Free-Molecular Regime," *J. Colloid Interf. Sci.*, **139**(1), 63 (1990).

Marchal, P., R. David, J. P. Klein, and J. Villermaux, "Crystallisation and Precipitation Engineering. I: An Effective Method for Solving the Population Balance for Crystallisation with Agglomeration," *Chem. Eng. Sci.*, **43**(1), 59 (1988).

Randolph, A. D., and M. A. Larson, *Theory of Particulate Processes*, 2nd. ed., , Academic Press (1988).

Smit, D. J., M. J. Hounslow, and W. R. Paterson, "Aggregation and Gelation I. Analytical Solution for Batch and Continuous Vessels," *Chem. Eng. Sci.*, **49**(7), 1025 (1994).

Zachariah, M. R., D. Chin, H. G. Semerjian, and J. L. Katz, "Dynamic Light-Scattering and Angular Dissymmetry for the in situ Measurement of Silicon Dioxide Particle Synthesis in Flames," *Appl. Opt.*, **28**(3), 530 (1989).

Appendix A

Proof that Eq. 35 satisfies Eq. 11:

$$\frac{dm_0}{dt} = \sum_i \frac{dN_i}{dt}$$

$$= \sum_i \left\{ \sum_{j=1}^{i-S(q)} \beta_{i,j} N_i N_j \frac{2^{(j-i)/q}}{2^{1/q}-1} \right. \tag{A1}$$

$$+ \sum_{k=2}^{q} \sum_{j=i-S(q-k+2)+1}^{i-S(q-k+1)}$$

$$\beta_{i,j} N_i N_j \frac{2^{(j-i+1)/q} + 2^{1/q} - 2^{k/q}}{2^{1/q}-1} \tag{A2}$$

$$+ \sum_{k=2}^{q} \sum_{j=i-S(q-k+2)+1}^{i-S(q-k+1)}$$

$$\beta_{i,j} N_i N_j \frac{-2^{(j-i)/q} + 2^{k/q} - 1}{2^{1/q}-1} \tag{A3}$$

$$+ \frac{1}{2} \beta_{i,i} N_i^2 \tag{A4}$$

$$- \sum_{j=1}^{i-S(q)} \beta_{i,j} N_i N_j \frac{2^{(j-i)/q}}{2^{1/q}-1} \tag{A5}$$

$$\left. - \sum_{j=i-S(q)+1}^{\infty} \beta_{i,j} N_i N_j \right\}. \tag{A6}$$

We note that

$$\text{term (A1)} + \text{(A5)} = 0.$$

Also,

$$\text{term (A2)} + \text{term (A3)} = \sum_{k=2}^{q} \sum_{j=i-S(q-k+2)+1}^{i-S(q-k+1)} \beta_{i,j} N_i N_j$$

$$= \sum_{j=i-S(q)+1}^{i-1} \beta_{i,j} N_i N_j.$$

Finally, combining all terms we get that

$$\frac{dm_0}{dt} = \sum_i \left(\frac{1}{2} \beta_{i,i} N_i^2 - \sum_{j=i}^{\infty} \beta_{i,j} N_i N_j \right).$$

Hounslow et al. (1988) show that for the size-independent kernel this becomes

$$\frac{dm_0}{dt} = -\frac{1}{2} \beta_0 m_0^2.$$

Appendix B

Proof that Eq. 35 satisfies Eq. 12, $dm_3/dt = 0$:

$$\frac{dm_3}{dt} = \sum_i \bar{v}_i \frac{dN_i}{dt}$$

$$= \sum_i \bar{v}_i \left\{ \sum_{j=1}^{i-S(q)} \beta_{i,j} N_i N_j \frac{2^{(j-i+1)/q}}{2^{1/q}-1} \right. \tag{B1}$$

$$+ \sum_{k=2}^{q} \sum_{j=i-S(q-k+2)+1}^{i-S(q-k+1)}$$

$$\beta_{i,j} N_i N_j \frac{2^{(j-i+1)/q} - 2^{k/q} + 2^{1/q}}{2^{1/q}-1} \tag{B2}$$

$$+ \sum_{k=2}^{q} \sum_{j=i-S(q-k+2)+1}^{i-S(q-k+1)}$$

$$\beta_{i,j} N_i N_j \frac{-2^{(j-i-k+1)/q} + 2^{1/q} - 2^{-(k-1)/q} - 1}{2^{1/q}-1} \tag{B3}$$

$$+ \frac{1}{2} \beta_{i,i} N_i^2 \tag{B4}$$

$$- \sum_{j=1}^{i-S(q)} \beta_{i,j} N_i N_j \frac{2^{(j-i)/q}}{2^{1/q}-1} \tag{B5}$$

$$\left. - \sum_{j=i-S(q)+1}^{\infty} \beta_{i,j} N_i N_j \right\}. \tag{B6}$$

Adding terms B1 and B5 yields

$$\frac{dm_3}{dt} = \sum_{j=1}^{i-S(q)} \beta_{i,j} N_i N_j 2^{(j-i)/q}. \tag{B7}$$

Terms B2 + B3 yields

$$\frac{dm_3}{dt} = \sum_{k=2}^{q} \sum_{j=i-S(q-k+2)+1}^{i-S(q-k+1)} \beta_{i,j} N_i N_j (2^{(j-i)/q} + 1)$$

$$= \sum_{j=i-S(q)+1}^{i-1} \beta_{i,j} N_i N_j (2^{(j-i)/q} + 1). \tag{B8}$$

Adding terms B4 and B6 to B7 and B8 yields

$$\frac{dm_3}{dt} = \sum_{j=1}^{i-1} \beta_{i,j} N_i N_j 2^{(j-i)/q} - \sum_{j=i+1}^{\infty} \beta_{i,j} N_i N_j.$$

Finally, we get that

$$\frac{dm_3}{dt} = \sum_i \bar{v}_i \left(\sum_{j=1}^{i-1} \beta_{i,j} N_i N_j 2^{(j-i)/q} - \sum_{j=i+1}^{\infty} \beta_{i,j} N_i N_j \right).$$

By noting that $\beta_{i,j} = \beta_{j,i}$ and $\overline{v_{i+1}}/\bar{v}_i = 2^{1/q}$, we obtain that

$$\frac{dm_3}{dt} = 0.$$

Manuscript received Nov. 15, 1993, and revision received Mar. 7, 1994.